Normalized performance parameters for a residential heat pump in the cooling mode with single faults imposed

CrossMark

Jin Min Cho [a], Jaehyeok Heo [b], W. Vance Payne [b],[*], Piotr A. Domanski [b]

[a] School of Mechanical and Aerospace Engineering, Seoul National University, Seoul 151-744, Republic of Korea
[b] HVAC&R Equipment Performance Group, National Institute of Standards and Technology, 100 Bureau Drive, MS 8631, Gaithersburg, MD 20899, USA

HIGHLIGHTS

- The effects of nine common faults on heat pump cooling performance were correlated.
- The correlation may be applied to determine the annual cost of an individual fault.
- The normalized correlation is applicable to residential style split heat pump systems.

ARTICLE INFO

ABSTRACT

The cooling mode performance of a residential split heat pump operating under nine different faults was described using normalized performance parameters determined from a ratio of the fault value to the no-fault value obtained from heat pump tests in environmental chambers. The normalized parameters were the coefficient of performance (COP), total capacity, refrigerant-side capacity, sensible heat ratio, outdoor unit power, and total power. A correlation for the normalized performance parameters was developed to produce a continuous representation of the performance characteristics given the fault level and indoor and outdoor temperature conditions.

Published by Elsevier Ltd.

1. Introduction

Fault detection and diagnostic (FDD) technology found its first applications in safety critical systems, e.g., nuclear power plants, airplanes. For safety non-critical systems, such as space-conditioning and refrigeration equipment, the interest in applying FDD has lagged until these technologies approach the threshold of economic viability. Reports of major studies on FDD for heating, ventilation and air-conditioning (HVAC) systems started to appear in the literature in the nineties, and the number of publications noticeably increased within the last ten years.

Table 1 lists a few examples of studies published since 2001. The majority of studies focused on analytical developments and provided limited performance data of systems operating under faults. The objective of this paper is to present global performance parameters of a residential heat pump operating in the cooling mode under single fault. These parameters are presented in a non-dimensional format; their values were calculated by dividing a value obtained under faulty operation to a fault-free value under the same operating condition. The paper also presents correlations, which express these non-dimensional parameters as a function of operating conditions and the fault level. The non-dimensional presentation of faulty performance facilitates a better understanding of performance degradation of a heat pump due to common faults. The non-dimensional correlations can also be used to estimate the increase in seasonal energy consumption and energy cost due to faults by performing seasonal simulations of a building equipped with a heat pump operating with a fault.

2. Laboratory measurements

2.1. Experimental apparatus

The experimental apparatus used in this study was described in detail by Kim et al. [6]. The studied system was a single-speed, split heat pump with an 8.8 kW rated cooling capacity. The heat pump was equipped with a thermostatic expansion valve (TXV). Fig. 1 shows a schematic diagram of the experimental setup with the locations of the main measurements. The air-side measurements included indoor dry-bulb and dew-point temperatures, outdoor

* Corresponding author. Tel.: +1 301 975 6663; fax: +1 301 975 8973.
   E-mail address: vance.payne@nist.gov (W.V. Payne).

Nomenclature

a	coefficient of multivariate polynomial
CF	improper outdoor air flow rate (condenser fouling) fault
CMF	compressor or four-way reversing valve leakage fault
COP	coefficient of performance
EF	improper indoor air flow rate (evaporator fouling) fault
F	fault level [% or dimensionless (fraction)]
FDD	fault detection and diagnosis
HVAC	heating, ventilating, air-conditioning equipment
LL	liquid line restriction fault
NC	presence of non-condensable gases fault
OC	refrigerant overcharge fault
P	pressure [Pa]
Q	capacity [W]
SC	refrigerant subcooling at the liquid line service valve [°C]
SHR	sensible heat ratio (sensible capacity divided by total capacity)
T	temperature [°C]
TXV	thermostatic expansion valve
UC	refrigerant undercharge fault
VOL	electric line voltage fault
W	power [W]
X or x	measured data or performance parameter
Y	normalized performance parameter

Greek symbols

α	function shown in Eq. 2
Δ	difference
φ	calculated data of performance parameter

Subscripts

i	feature index
ID	indoor dry-bulb
IDP	indoor dew-point
OD	outdoor dry-bulb
ODU	outdoor unit
sat	saturation
tot	total

---

dry-bulb temperature, barometric pressure, and pressure drop across the air tunnel (not shown on the schematic). T-type thermocouple grids and thermopiles with twenty-five nodes measured air temperatures and temperature change, respectively. On the refrigerant side, pressure transducers and T-type thermocouple probes measured the inlet and exit parameters at every component of the system.

Table 2 lists uncertainties of the major quantities measured. For a complete uncertainty analysis the reader can refer to Kim et al. [6].

2.2. Studied faults and their implementation

Table 3 lists nine studied faults, including their definition and range. The majority of heat pump measurements for these faults were taken and reported by Kim et al. [6]. For the purpose of this study, we conducted additional tests on the same equipment and test apparatus, specifically for the improper electric line voltage fault and improper liquid line refrigerant subcooling fault, which were not studied by Kim et al. [6]. Also, additional tests were performed for a few other faults to expand their range to those listed in Table 3.

The compressor valve leakage fault and the four-way valve leakage fault are considered together because they have a similar effect on the heat pump performance by reducing the refrigerant mass flow rate through the system. In a compressor, a leak can

occur at the suction or discharge valves for the reciprocating type, or between the high-pressure and low-pressure portions of the scroll design. The four-way valve can leak from the hot gas, high-pressure side to the low-pressure, suction gas passages. In this study, the compressor/four-way valve leakage fault was implemented using a hot gas bypass from the discharge to the suction of the compressor, and the fault level was defined as the ratio of change in refrigerant mass flow rate to the no-fault refrigerant mass flow rate. With this definition, a complete loss of refrigerant mass flow rate would correspond to the 100% fault level.

The outdoor and indoor air flow faults can be caused by coil fouling. The outdoor air flow fault was implemented by blocking portions of the outdoor heat exchanger face area with paper sheets; the ratio of blocked area to total area determined the fault level, with the −100% fault level indicating total blockage. The indoor air flow fault was implemented by lowering the speed of the nozzle chamber booster fan to increase the external static pressure across the indoor air handler. The fault level was calculated as a ratio of the fault-imposed air mass flow rate to the no-fault air mass flow rate, with the −100% fault level indicating a complete loss of air flow.

A liquid line restriction fault can be caused by a dirty refrigerant filter/dryer or by a kinked liquid line. This fault was implemented by closing a throttling valve installed in the liquid refrigerant line. The fault level was calculated as a ratio of the pressure difference between the liquid line service valve located at the condenser exit and the indoor TXV to the no-fault pressure differential. With this

Table 1
Selected studies on FDD.

| Investigator(s)	System type	Study focus
Comstock and Braun [1]	Centrifugal chiller	Experiment, eight single faults
Kim et al. [2,3]	Residential heat pump	Experiment for cooling mode, single-faults diagnosed with rule-based chart
Chen and Braun [4]	Rooftop air-conditioner	Simplified rule-based chart method
Navarro-Esbri et al. [5]	General vapor compression system	Dynamic model based FDD for real-time application
Kim et al. [6,7]	Single-speed, residential heat pump	Single-faults and steady-state detector study
Wang et al. [8]	HVAC system for new commercial buildings	System-level FDD involving sensor faults
Cho et al. [9]	Air-handling unit for buildings	Multiple faults
Li and Braun [10]	Direct expansion vapor compression system	Multiple faults
Du and Jin [11]	Air handling unit	Multiple faults
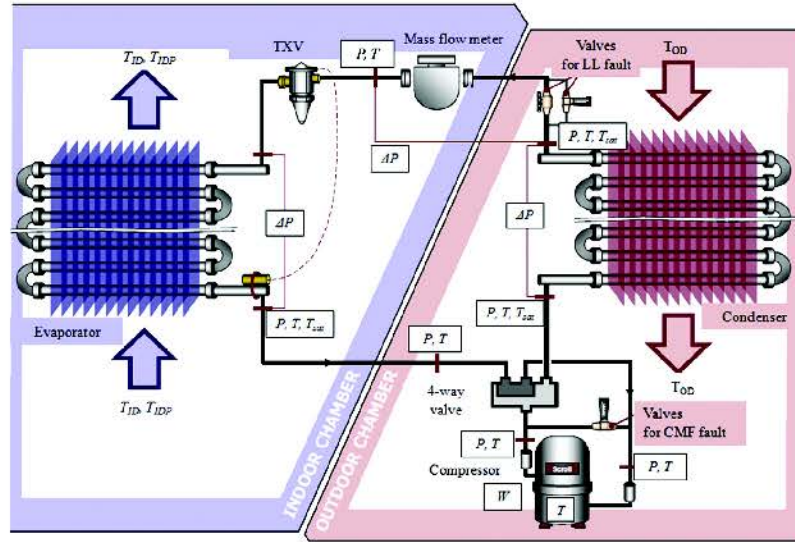
Fig. 1. Schematic diagram of experimental apparatus [6].

definition, the 100% fault level corresponds to a doubled pressure drop.

The no-fault refrigerant charge was set in the cooling mode at the standard A-Test condition [12] according to manufacturer instructions. The refrigerant undercharge and overcharge faults were implemented by adding or removing the refrigerant from a correctly charged system. The fault level was defined as the ratio of the refrigerant mass by which the system was overcharged or undercharged to the no-fault refrigerant charge, with 0% indicating the correct, no-fault charge, −100% indicating no refrigerant charge, and 100% indicating doubled charge.

The amount of refrigerant in a TXV-equipped system can also be estimated by examining the refrigerant subcooling in the liquid line; this method is commonly used by field technicians installing or servicing a heat pump. Therefore, we also characterized the effect of refrigerant overcharge by noting the liquid line subcooling at increased charge levels. The ratio of fault-imposed subcooling to the no-fault subcooling indicated the fault level with the 0% fault corresponding to the proper subcooling, and the 100% fault indicating a doubled subcooling level.

The non-condensable gas fault is caused by incomplete evacuation of the system during installation or after a repair that required opening the system to the atmosphere. When a new heat pump is installed, the outdoor unit is typically pre-charged, and the installer needs to evacuate the indoor section and the connecting line set before charging it with refrigerant. A common recommendation is to evacuate the system to a vacuum of 500 μPa [13]. The non-condensable gas fault was implemented by adding dry nitrogen

Table 2
Measurement uncertainties.

Measurement	Measurement range	Uncertainty at the 95% confidence level
Air temperature	10 °C—93 °C	±0.3 °C
Air temperature difference	0 °C—28 °C	±0.3 °C
Air nozzle pressure	0 Pa−1245 Pa	±1.0 Pa
Refrigerant mass flow rate	0 kg/h−544 kg/h	±1.0%
Dew-point temperature	0 °C−38 °C	±0.4 °C
Dry-bulb temperature	0 °C−40 °C	±0.4 °C
Cooling capacity	3 kW−11 kW	±4.0%
COP	2.5−6.0	±5.5%

to the evacuated system before the charging process. This fault level is defined by the ratio of pressure in the evacuated indoor section due to non-condensable to the atmospheric pressure. The 0% fault level occurs when the refrigerant charging process starts with a vacuum, and the 100% fault level would occur when the nitrogen filled refrigerant lines are at atmospheric pressure before the refrigerant is charged.

The electrical line voltage fault was implemented by varying the supply voltage to the system from the nominal, no-fault value of 208 VAC. The fault level was defined by the percentage by which the line voltage was above or below the nominal level, with a positive fault indicating a voltage above 208 VAC.

3. Fault effects on heat pump performance

3.1. Normalized performance parameters and correlation

The study considered the effect of faults on six performance parameters: coefficient of performance (COP), total cooling capacity (Q_{tot}, net capacity accounting for indoor fan heat), refrigerant-side cooling capacity (Q_R, capacity does not include the indoor fan heat), sensible heat ratio (SHR), outdoor unit power (W_{ODU}, which included the compressor, outdoor fan, and controls power), and total power (W_{tot}). These parameters are presented in a dimensionless, normalized format obtained by dividing these dimensional parameter values as obtained for the heat pump operating under a selected fault to the no-fault value of a given performance parameter obtained for the heat pump operating fault free. The normalized parameters were correlated as a function of the indoor dry-bulb temperature (T_{ID}), outdoor dry-bulb temperature (T_{OD}), and fault level (F), as given in Eq. (1).

$$Y = \frac{X_{fault}}{X_{no-fault}} \quad (1)$$

$$Y = \alpha F + 1, \quad \alpha = f(T_{ID}, T_{OD}, F) \quad (2)$$

where X_{fault} and $X_{no-fault}$ are dimensional performance parameters for a faulty and fault-free heat pump, and Y is a dimensionless parameter representing the ratio of the faulty performance to that

Table 3
Definition and range of studied faults.

Fault name	Symbol	Definition of fault level	Fault range (%)
Compressor valve leakage (4-way valve leakage)	CMF	% reduction in refrigerant flow rate from no-fault value	0–40 (F = 0–0.40)
Reduced outdoor air flow rate (condenser fouling)	CF	% of coil area blocked	−30–0 (F = −0.30–0)
Improper indoor air flow rate (evaporator fouling)	EF	% above or below correct air flow rate	−50–20 (F = −0.50–0.20)
Liquid line restriction	LL	% change from no-fault pressure drop from liquid line service valve to indoor TXV inlet	0–32 (F = 0–0.32)
Refrigerant undercharge	UC	% mass below correct (no-fault) charge	−30–0 (F = −0.30–0)
Refrigerant overcharge	OC	% mass above correct (no-fault) charge	0–30 (F = 0–0.30)
Presence of non-condensable gases	NC	% of pressure in evacuated indoor section and line set, due to non-condensable gas, with respect to atmospheric pressure	0–20 (F = 0–0.20)
Improper electric line voltage	VOL	% above or below 208 V	−8.7–25 (F = −0.087–0.25)
Improper liquid line refrigerant subcooling	SC	% above the no-fault subcooling value	0–200 (F = 0–2.00)

of the fault-free heat pump. When the system is fault-free, fault level equals to zero and the normalized Y should have the value of one. Therefore, the correlation for Y must have a multiplication term with fault level and y-intercept of one as given in Eq. (2). The value of alpha also can vary with the operating conditions and fault levels so that alpha should be a function of T_{ID}, T_{OD}, and F as given in Eq. (2). In this paper, the correlation for alpha was chosen as a first order multivariable polynomial equation as given in Table 4. Co-efficients were determined by means of a multivariate polynomial regression method using the normalized values of performance parameters determined from heat pump test data. If the heat pump is fault free, values of all normalized parameters equal unity.

The fit standard error of the normalized correlation variable, Y, was a maximum of 3% over the range of operating conditions listed in Table 5. An example calculation using the 3% uncertainty in Y and the equations listed in Table 4 showed a propagation of uncertainty for the faulty COP and cooling capacity as listed in Table 5. All correlations listed in Table 4 should be used with caution if extrapolating outside of the temperature ranges listed in Table 5.

3.2. Charts with normalized performance parameters

Fig. 2–10 show variation of the normalized performance parameters with respect to fault levels at five different operating conditions. The figures present the measured data points and correlations developed for COP, total capacity, refrigerant-side capacity, SHR, the outdoor unit power, and total power. Each correlation has the multivariable term such as T_{ID}, T_{OD}, and F, so that it covers all driving conditions.

In some of the figures there is significant difference between the correlation fits and the actual data points. The correlation was performed for all indoor and outdoor test conditions and thus the fit sum of squared deviations was minimized. In addition, the value for the heat pump operating with no fault was calculated from the fault-free correlation as presented by Kim et al. [14], because the performance value with no fault measured at a certain driving condition cannot represent those at all driving conditions. This is the reason why the 0% values have a little spread in most figures. A departure from the correlation is obvious, but the correlation still follows the general performance trends at all fault levels. For a more general correlation of normalized performance, fault level could be used as the only independent variable while still capturing the general effects of the faults on system performance; in general, Y varies linearly with fault level, F.

Fig. 2 presents the normalized parameters for the compressor valve leakage fault, which reduces the refrigerant flow rate through the heat exchangers. The effect of this fault on system performance parameters is substantial and does not vary markedly between different operating conditions. At 10% fault level, the COP and capacity degradation were approximately 10% while the outdoor unit

power decrease was within 3%. The sensible heat ratio increased by approximately 5% because the suction pressure increased thus increasing the evaporator saturation temperature, increasing the evaporator surface temperature and decreasing latent capacity. Although the figures include data points for fault levels of up to 40% for one of the operating conditions, a more realistic fault level that could be observed in the field is up to 10%, unless the four way refrigerant reversing valve failed to operate properly and provided a large path for refrigerant leakage from the high pressure to low pressure side.

Fig. 3 shows the normalized performance parameters for a reduced outdoor air flow fault. When the blocked area is increased to 30%, the degradation in COP is between 10% and 13%, depending on the operating condition. When this fault occurs, the air-side heat transfer coefficient is reduced and the air temperature change across the condenser is increased, which raises the pressure in the condenser, increases the compressor power and reduces refrigerant mass flow rate. Hence, the decrease in COP for this fault is a result of both a decrease in the capacity and an increase in total power.

Fig. 4 shows the normalized parameters at a reduced and increased indoor air flow. For the studied air flow range from −50% to 20% of the nominal value, the change in outdoor unit power ranged from −3% to 0%, respectively, with small variations between different operating conditions. Total power varied from −5% to 2% within the same range of air flow rate, which indicates the varied power of the indoor fan at this fault. COP and capacity were markedly degraded at a decreased air flow and somewhat improved at the increased air flow above the nominal level; however, these increases in COP and capacity are associated with a significant increase in SHR, which may not be a desirable change from the homeowner's comfort point of view. The difference between total power and outdoor unit power is due to the power of the indoor blower, which was nominally 430 W. Outdoor unit power was relatively constant under this fault. As a result, COP slightly increased at the max fault level by the increased indoor air flow.

Fig. 5 shows the variation of the normalized values for chosen performance parameters for various LL fault levels. Due to the actions of the TXV, self-compensation is apparent from no-fault to 10% fault level. However, COP and total capacity showed a relatively large degradation as the fault level exceeded 20% in spite of TXV operation.

Figs. 6 and 7 show the variation of the normalized values for refrigerant charge faults. The degradation in COP and total capacity for refrigerant undercharge are larger than those for refrigerant overcharge. A 30% undercharge reduced capacity by almost 15% on average reducing COP by 12% while a 30% overcharge produced little-reductions or small increases in capacity with 6% greater total power and 3% reduced COP on average because of the increased discharge pressure. In case of different outdoor temperature conditions, COP and capacity increased as the outdoor temperature

Table 4
Correlations for non-dimensional performance parameters.

Fault	Performance parameter	$Y = 1 + (a_1 + a_2T_{ID} + a_3T_{OD} + a_4F)\cdot F$				FSE[a]
		a_1	a_2	a_3	a_4	
Compressor leakage (CMF)	COP	$Y_{COP} = Y_{Q_{tot}}/Y_{W_{tot}}$				8.88E-03
	Q_{tot}	-1.12E+00	1.75E-02	-1.00E-02	1.56E-02	7.23E-03
	Q_R	-1.19E+00	1.24E-02	-6.03E-03	4.84E-02	4.58E-03
	SHR[b]	-2.00E-01	1.89E-02	5.45E-03	5.91E-01	4.42E-03
	W_{ODU}	6.98E-01	-2.66E-02	-8.18E-03	-1.30E-02	4.96E-03
	W_{tot}	6.35E-01	-2.51E-02	-7.81E-03	1.03E-01	5.15E-03
Improper outdoor air flow rate (CF)	COP	$Y_{COP} = Y_{Q_{tot}}/Y_{W_{tot}}$				1.80E-02
	Q_{tot}	-2.39E-01	8.95E-03	1.44E-03	-6.43E-01	1.16E-02
	Q_R	-2.71E-01	1.73E-02	-2.07E-03	-5.76E-01	1.20E-02
	SHR[b]	9.74E-02	-5.30E-03	8.39E-05	2.95E-01	4.93E-03
	W_{ODU}	1.51E-01	-8.83E-03	7.82E-03	1.34E+00	1.75E-02
	W_{tot}	1.29E-01	-5.58E-03	5.82E-03	1.15E+00	1.38E-02
Improper indoor air flow rate (EF)	COP	$Y_{COP} = Y_{Q_{tot}}/Y_{W_{tot}}$				1.63E-02
	Q_{tot}	1.85E-01	1.77E-03	-6.40E-04	-2.77E-01	1.53E-02
	Q_R	2.95E-01	-1.17E-03	-1.57E-03	6.92E-02	5.39E-03
	SHR[b]	5.93E-02	5.16E-03	1.81E-03	-2.89E-01	9.82E-03
	W_{ODU}	-1.03E-01	4.12E-03	2.38E-03	2.10E-01	6.91E-03
	W_{tot}	1.35E-02	2.95E-03	-3.66E-04	-5.88E-02	5.68E-03
Liquid line restriction (LL)	COP	$Y_{COP} = Y_{Q_{tot}}/Y_{W_{tot}}$				1.28E-02
	Q_{tot}	5.67E-01	-2.42E-02	1.24E-02	-2.81E+00	1.16E-02
	Q_R	3.78E-01	-1.90E-02	1.33E-02	-3.11E+00	1.58E-02
	SHR[b]	-7.09E-01	3.10E-02	-8.35E-03	1.09E+00	1.13E-02
	W_{ODU}	4.84E-01	-1.22E-02	-3.16E-03	-3.02E-01	6.05E-03
	W_{tot}	4.08E-01	-1.24E-02	-2.67E-03	-9.92E-02	5.50E-03
Refrigerant undercharge (UC)	COP	$Y_{COP} = Y_{Q_{tot}}/Y_{W_{tot}}$				1.15E-02
	Q_{tot}	-5.45E-01	4.94E-02	-6.98E-03	-1.78E-01	1.02E-02
	Q_R	-9.46E-01	4.93E-02	-1.18E-03	-1.15E+00	1.44E-02
	SHR[b]	4.19E-01	-2.12E-02	1.26E-03	1.39E-01	8.56E-03
	W_{ODU}	-3.13E-01	1.15E-02	2.66E-03	-1.16E-01	5.14E-03
	W_{tot}	-2.54E-01	1.12E-02	2.06E-03	5.74E-03	5.29E-03
Refrigerant overcharge (OC)	COP	$Y_{COP} = Y_{Q_{tot}}/Y_{W_{tot}}$				2.03E-02
	Q_{tot}	4.72E-02	-1.41E-02	7.93E-03	3.47E-01	1.96E-02
	Q_R	-1.63E-01	1.14E-02	-2.10E-04	-1.40E-01	5.67E-03
	SHR[b]	-7.75E-02	7.09E-03	-1.93E-04	-2.76E-01	7.34E-03
	W_{ODU}	2.19E-01	-5.01E-03	9.89E-04	2.84E-01	5.17E-03
	W_{tot}	1.46E-01	-4.56E-03	9.17E-04	3.37E-01	5.43E-03
Non-condensable gas (NC)	COP	$Y_{COP} = Y_{Q_{tot}}/Y_{W_{tot}}$				1.74E-02
	Q_{tot}	2.77E-01	−1.75E-02	1.78E-02	−1.96E+00	1.63E-02
	Q_R	-1.78E+00	4.04E-02	1.78E-02	9.98E-01	9.59E-03
	SHR[b]	-4.67E-01	1.69E-02	9.89E-04	2.90E-01	5.59E-03
	W_{ODU}	-6.92E-01	2.01E-02	1.20E-02	6.62E-01	6.13E-03
	W_{tot}	-5.37E-01	1.52E-02	1.09E-02	4.36E-01	6.20E-03
Improper line voltage (VOL)	COP	$Y_{COP} = Y_{Q_{tot}}/Y_{W_{tot}}$				1.95E-02
	Q_{tot}	5.84E-01	-1.21E-02	-8.57E-03	-3.35E-01	1.80E-02
	Q_R	1.03E-01	-6.10E-03	3.64E-03	-1.04E-01	6.41E-03
	SHR[b]	-6.65E-02	5.21E-03	-2.10E-03	4.23E-02	2.95E-02
	W_{ODU}	7.66E-01	-3.85E-03	-1.83E-02	1.14E+00	4.39E-03
	W_{tot}	9.06E-01	-6.37E-03	-1.75E-02	1.10E+00	7.39E-03
Improper liquid line refrigerant subcooling (SC)	COP	$Y_{COP} = Y_{Q_{tot}}/Y_{W_{tot}}$				2.26E-02
	Q_{tot}	6.77E-02	0.00E+00	-1.22E-03	-1.91E-02	2.18E-02
	Q_R	4.16E-02	0.00E+00	-3.51E-04	-1.55E-02	1.39E-02
	SHR[b]	-9.04E-02	0.00E+00	2.13E-03	1.60E-02	3.06E-02
	W_{ODU}	2.11E-02	0.00E+00	-4.18E-04	4.25E-02	4.34E-03
	W_{tot}	1.06E-02	0.00E+00	-2.93E-04	3.88E-02	4.84E-03

[a] FSE (fit standard error) equals the square root of the sum of the squared error divided by the degrees of freedom.
[b] The applicable range of SHR for wet coil predictions: 0.7 to 0.85.

increased for the undercharged condition. Farzad et al. [15] also showed that higher refrigerant flow rate is one reason for the higher capacity at higher outdoor temperatures for the conditions of undercharge.

Fig. 8 shows the variation of the normalized values for chosen performance parameters versus non-condensable gas (NC) fault level. Non-condensable gases increase the condensing pressure above that corresponding to the saturation pressure of the refrigerant at the same temperature due to the partial pressure of the NC components. As a result, increased total power consumption and decreased COP can be seen in Fig. 8. Maximum degradation of COP

at the 20% fault level was about 5% for the condition of $T_{ID} = 26.7$ °C and $T_{OD} = 27.8$ °C.

Fig. 9 shows the variation of the normalized values for chosen performance parameters for the line voltage variation fault conditions. A line voltage of 208 V was set as the no-fault condition. Total external static pressure for the indoor air handler was set at 125 Pa at the no-fault line voltage which produced a nominal indoor fan power demand of 430 W. As voltage increased, fan speed and static pressure increased thus producing increased fan power. Total power consumption increased almost linearly as fault level increased. The fan power increased more than the compressor

Table 5
Operating conditions and example uncertainty in *Y*.

Measurement	Operating range
Indoor air temperature	20 °C—27 °C
Indoor dewpoint temperature	10 °C—16 °C
Outdoor air temperature	20 °C—40 °C

Example uncertainty due to normalized correlation (*Y*) uncertainty of 3% for faulty COP and capacity at AHRI B-test conditions		
	Faulty value	Uncertainty
COP w/10% low indoor air flow	3.67	±6.4%
Cooling capacity w/10% low indoor air flow	9.4 kW	±5.0%
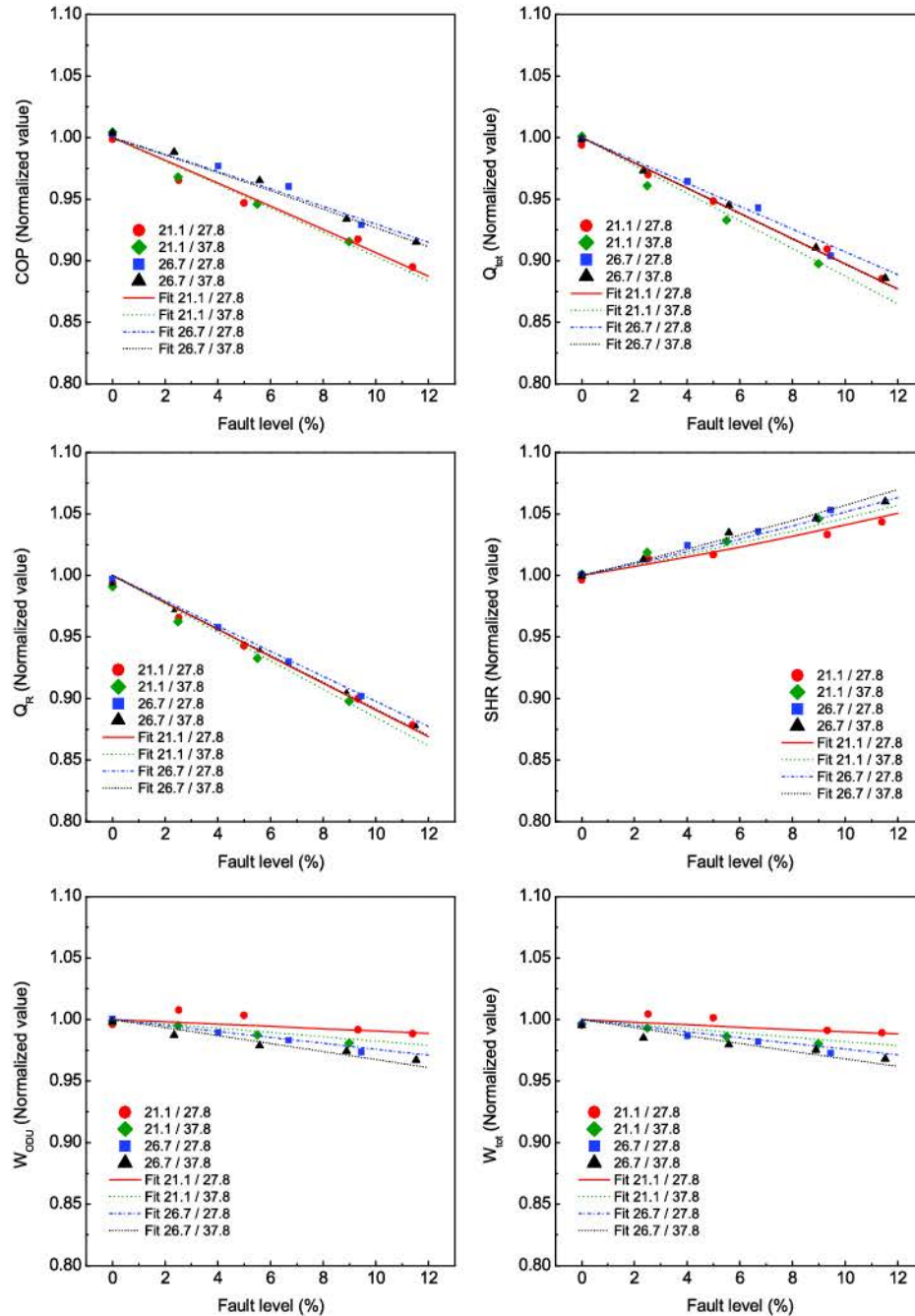
Fig. 2. Normalized performance parameters for compressor valve leakage (The numbers in the legend denote test conditions, T_{ID} (°C)/T_{OD} (°C)).
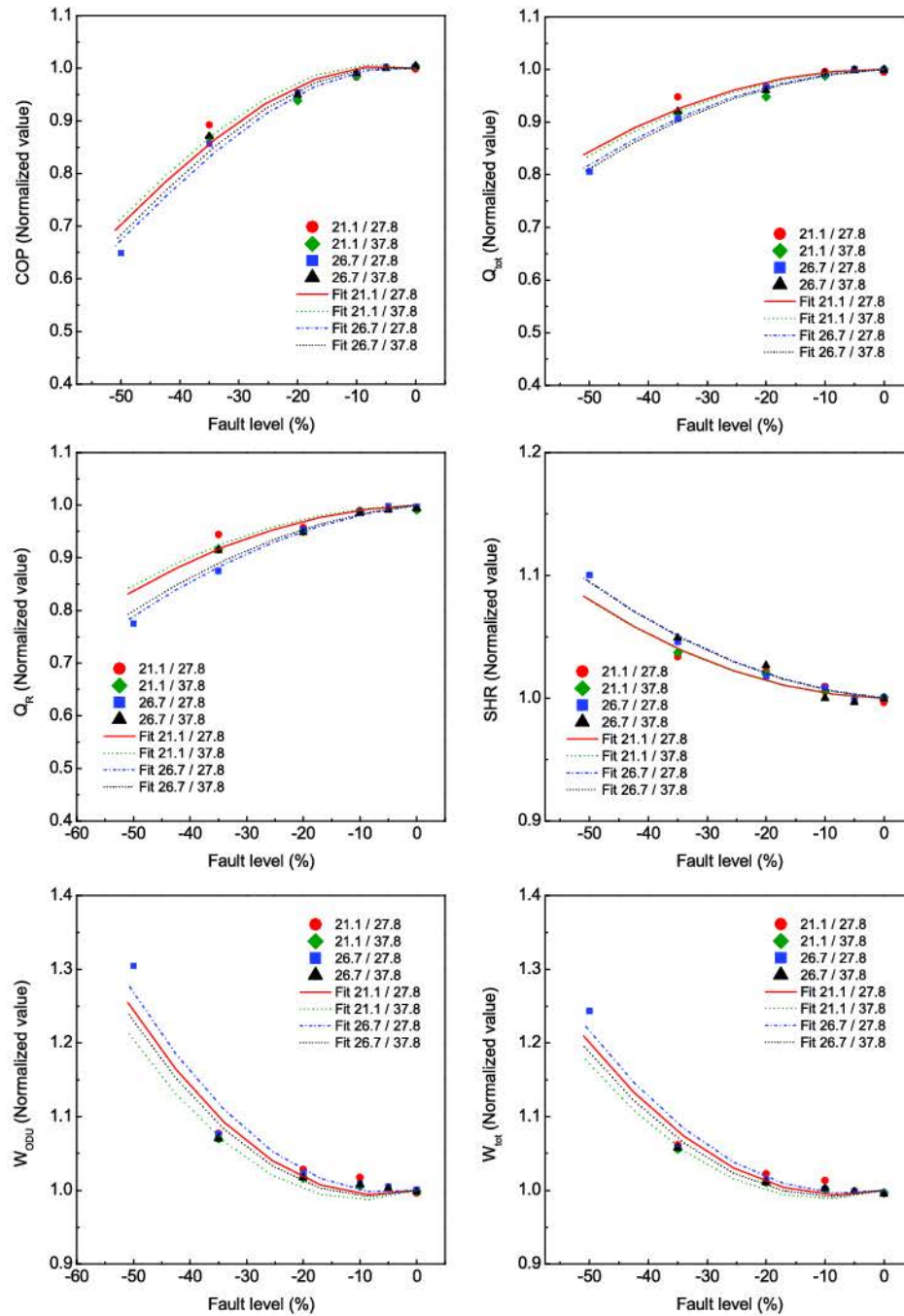
Fig. 3. Normalized performance parameters for reduced outdoor heat exchanger area (condenser fouling) (The numbers in the legend denote test conditions, T_{ID} (°C)/T_{OD} (°C)).

power when the voltage was increased. Average 27% of the fan power and 9% of the compressor power were increased at the max fault level. At over 20% fault levels, the degradation of COP is greater than 10%.

In this study, a subcooling temperature of 4.4 °C was regarded as the no-fault condition under the considered test conditions. Sub-cooling temperature change affected total system power consumption as shown in Fig. 10. The departure of the normalized values of COP and cooling capacity from the correlations in Fig. 10 are mostly due to the TXV attempting to correct mass flow rate (reduce

effective orifice size) as subcooling increases. If more data were available with subcooling being varied randomly from high to low values, hysteresis effects and TXV hunting effects would be better captured. COP and capacity normalized correlations for higher levels of subcooling still represent the general trends in system perfor-mance. The normalized values of COP indicated over 10% degrada-tion, and over 10% more total power was consumed at the maximum fault level of 181%. Increased subcooling has the same effect as increased refrigerant charge; higher subcooling leads to reduced condensing area and increased condensing pressure. As with
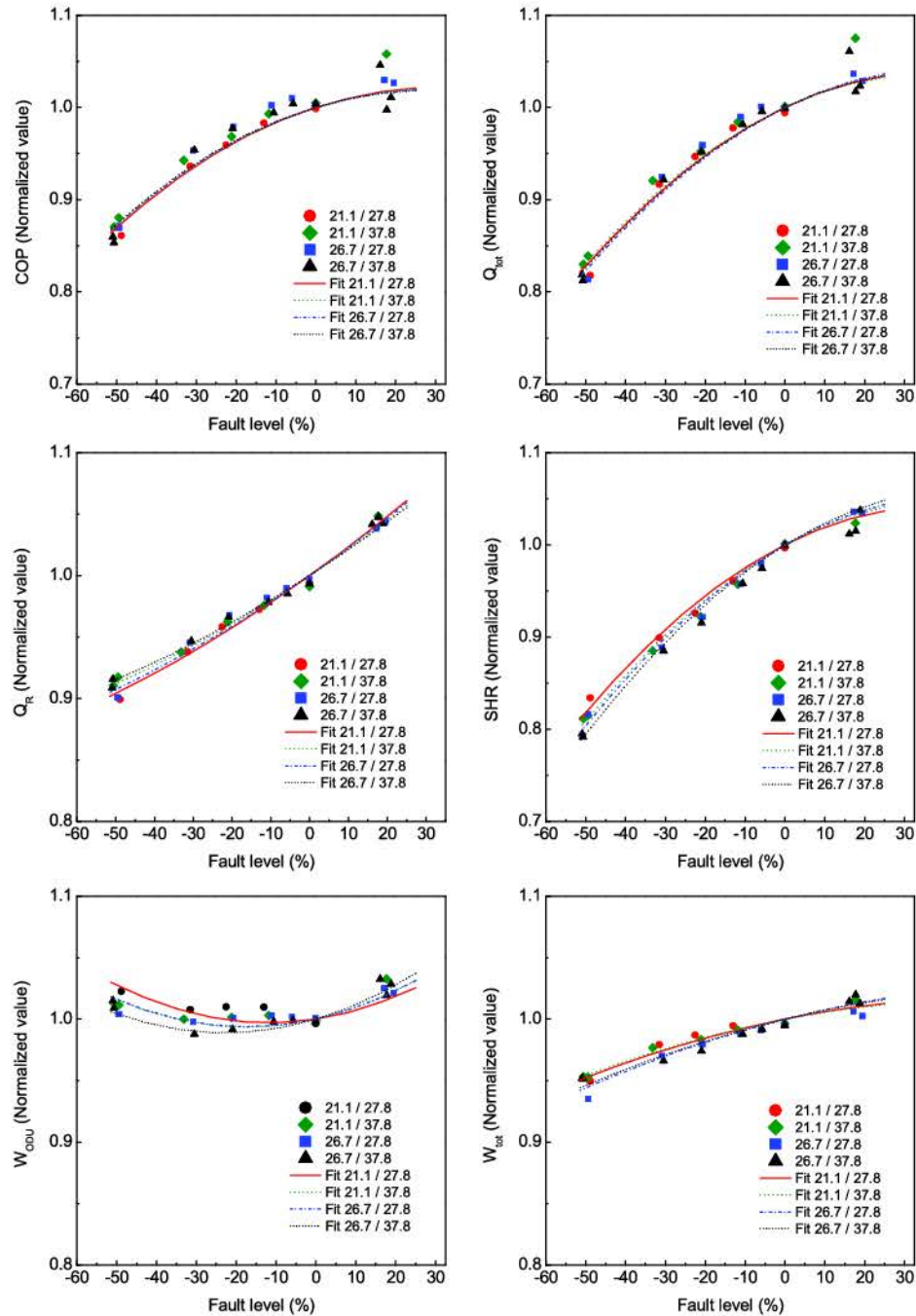
Fig. 4. Normalized performance parameters for improper indoor air flow (evaporator fouling) (The numbers in the legend denote test conditions, T_{ID} (°C)/T_{OD} (°C)).
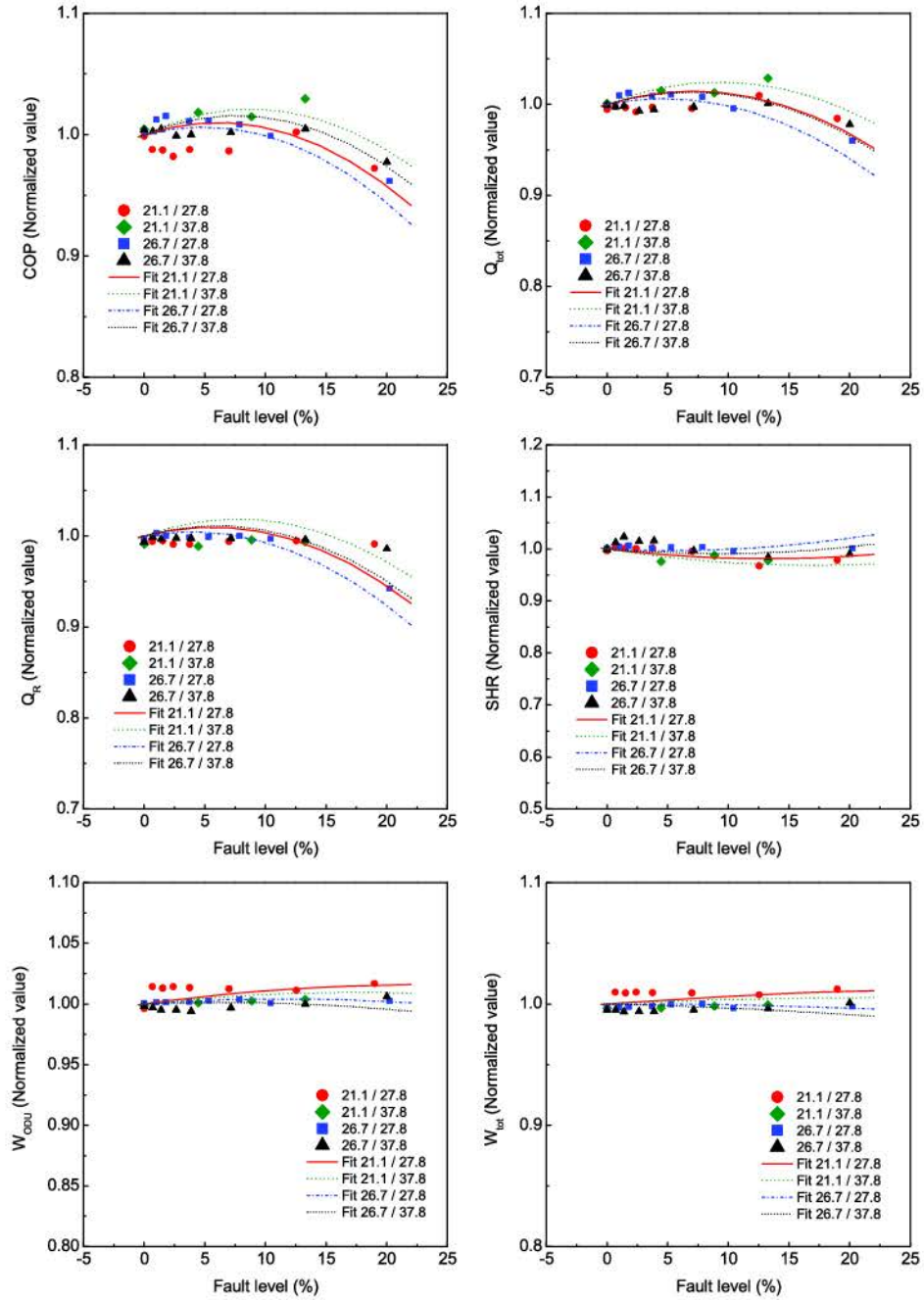
Fig. 5. Normalized performance parameters for liquid line restriction (The numbers in the legend denote test conditions, T_{ID} (°C)/T_{OD} (°C)).
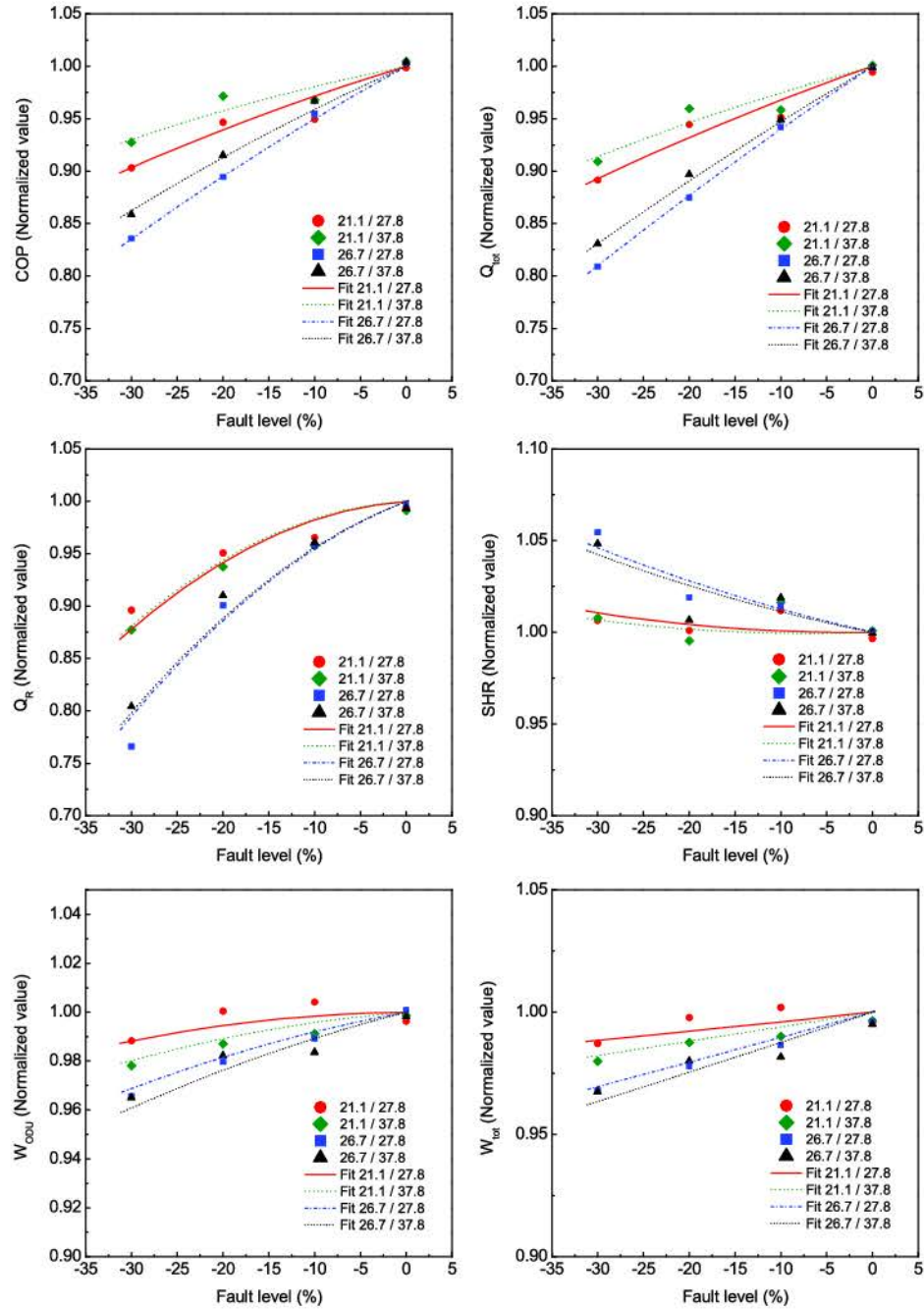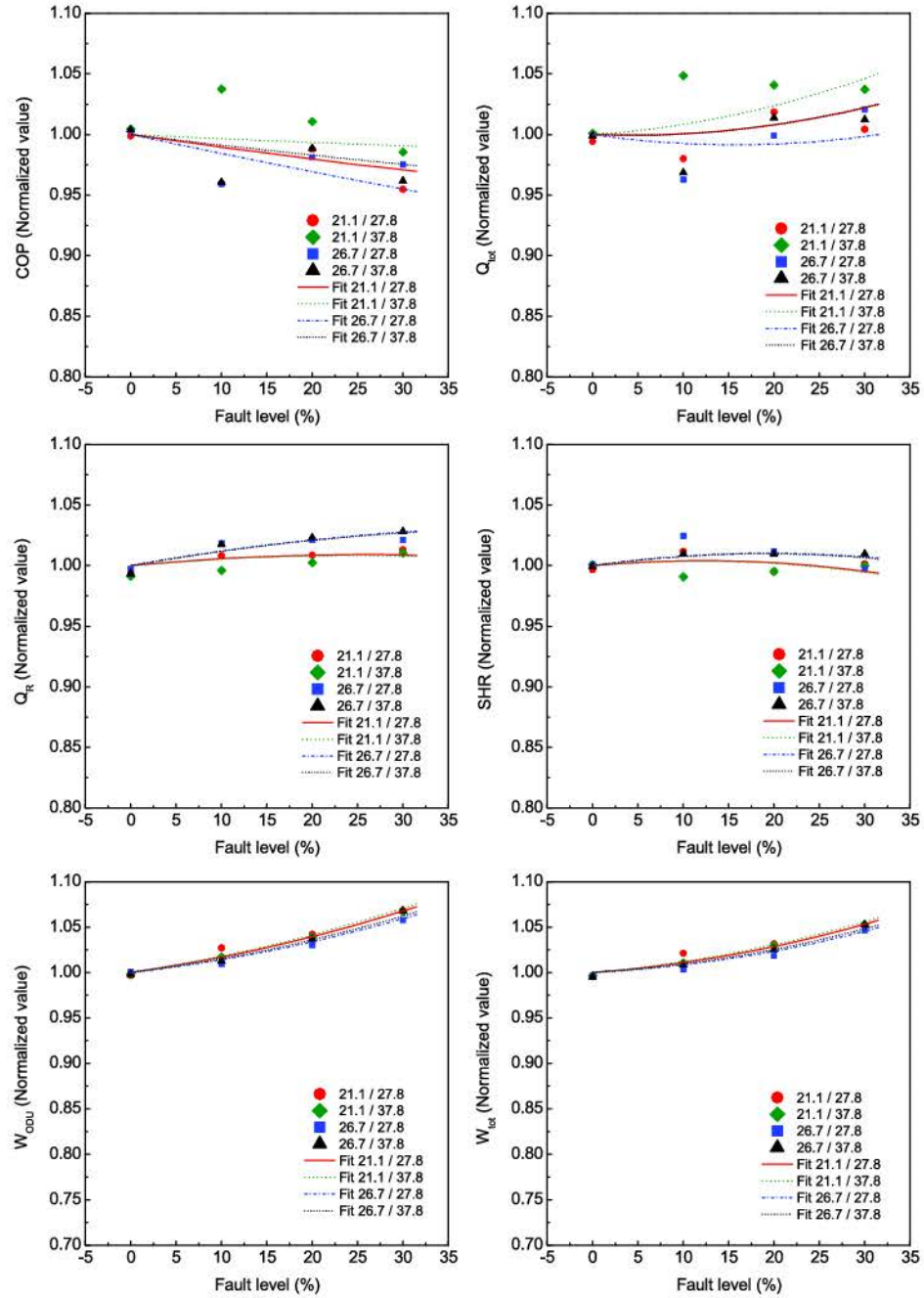
Fig. 6. Normalized performance parameters for refrigerant undercharge (The numbers in the legend denote test conditions, T_{ID} (°C)/T_{OD} (°C)).
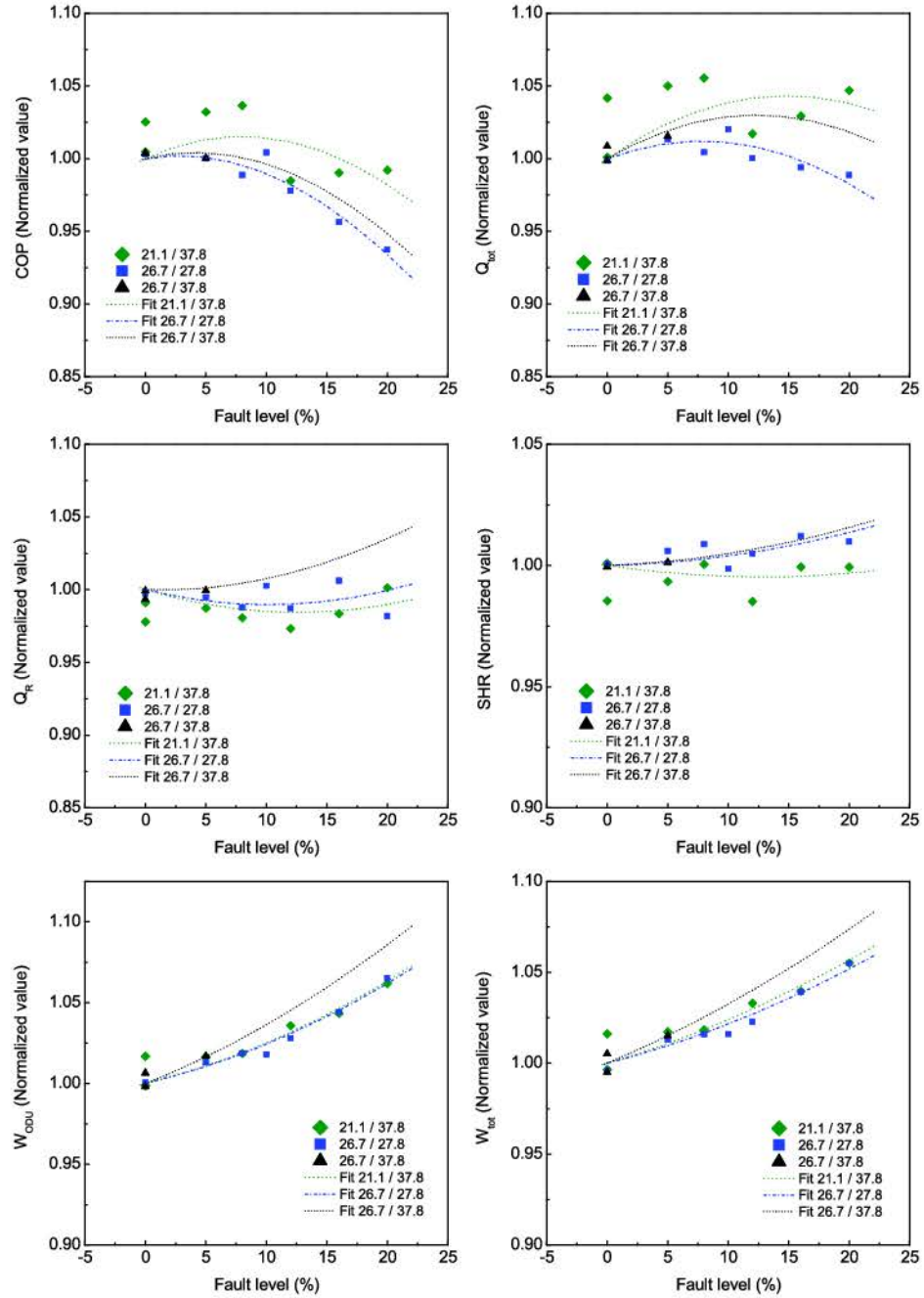
Fig. 7. Normalized performance parameters for refrigerant overcharge (The numbers in the legend denote test conditions, T_{ID} ($^\circ$C)/T_{OD} ($^\circ$C)).

Fig. 8. Normalized performance parameters for the presence of non-condensable gas (The numbers in the legend denote test conditions, T_{ID} (°C)/T_{OD} (°C)).
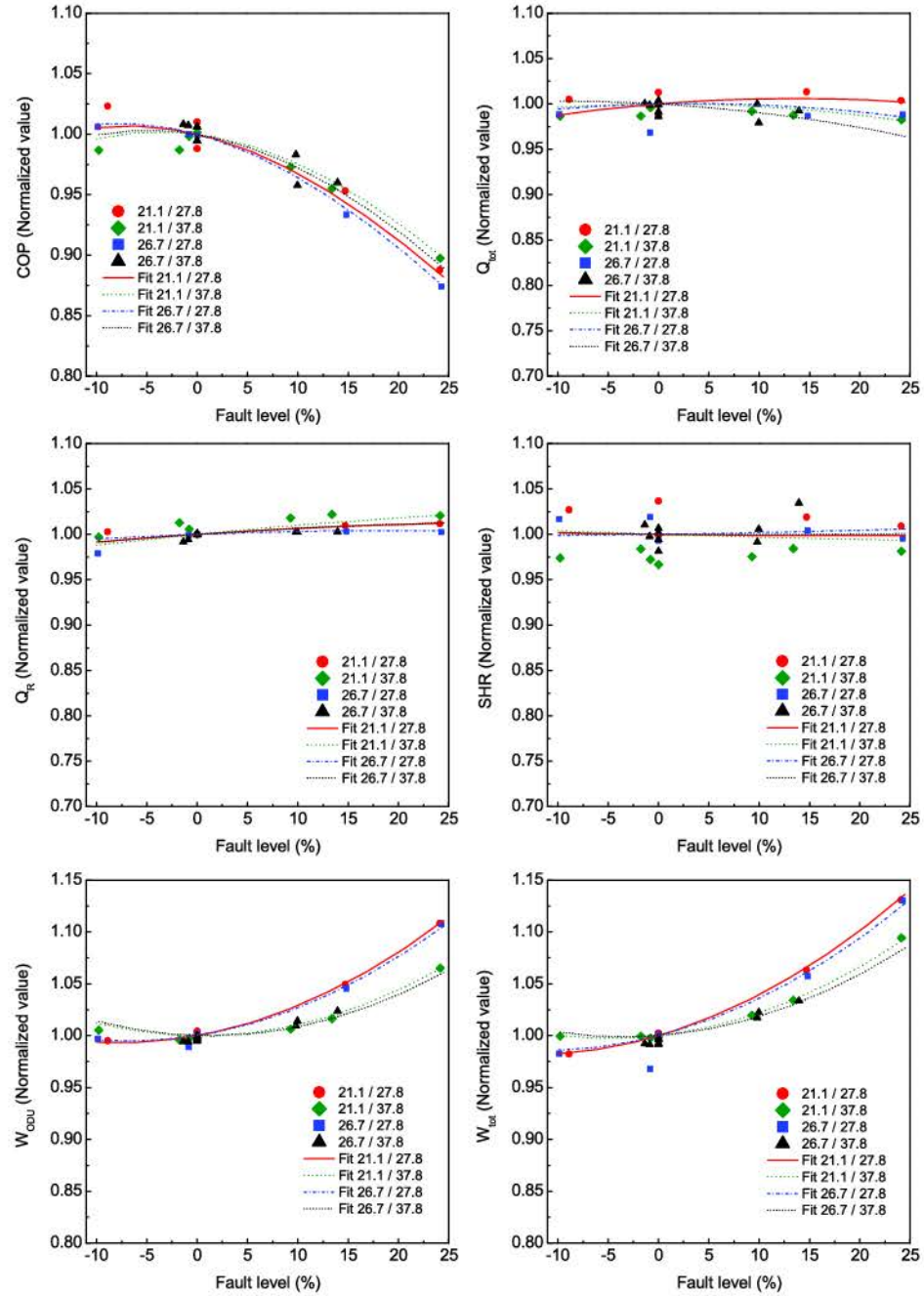
Fig. 9. Normalized performance parameters for improper electric line voltage (The numbers in the legend denote test conditions, T_{ID} (°C)/T_{OD} (°C)).
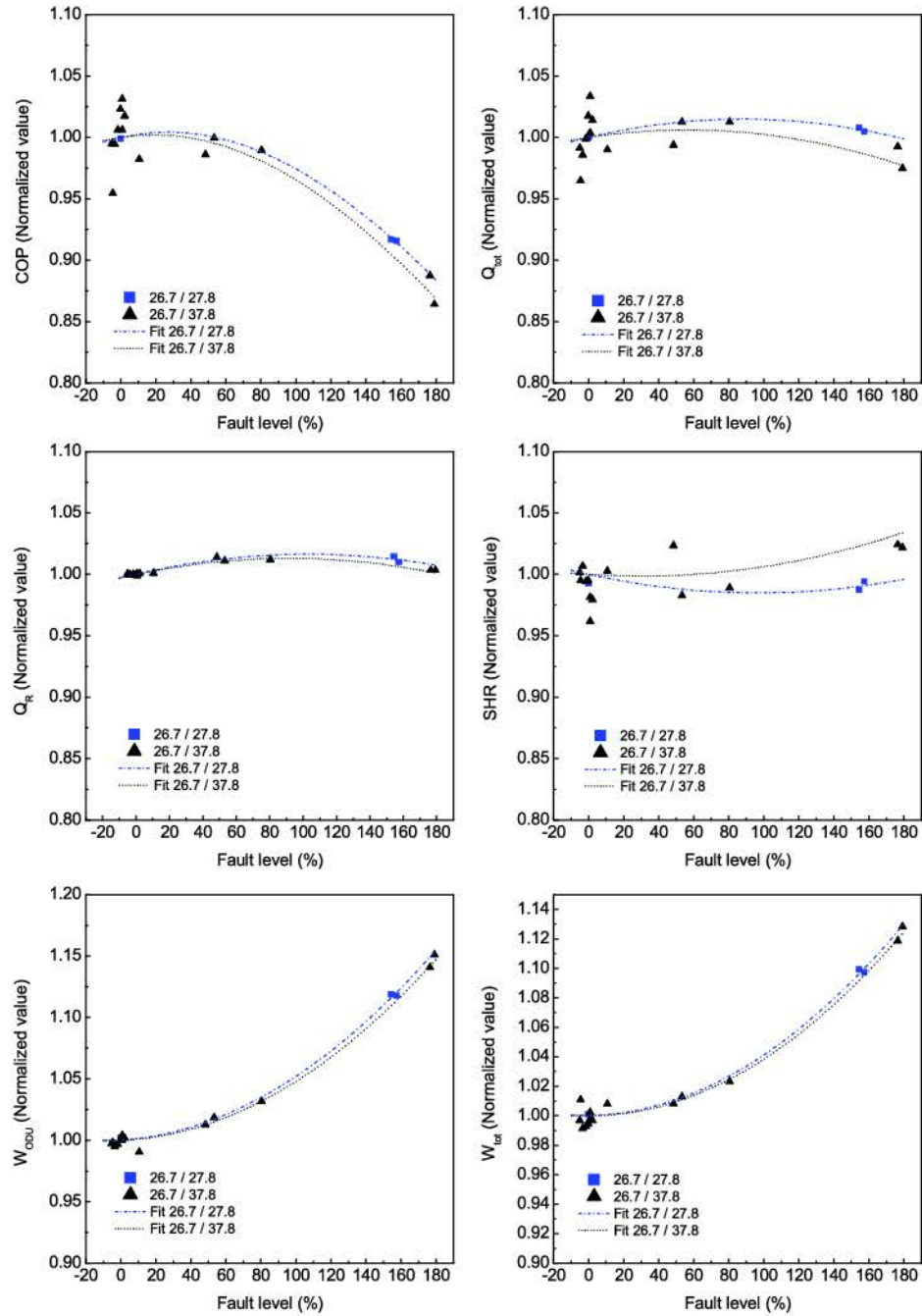
Fig. 10. Normalized performance parameters for improper liquid line refrigerant subcooling (The numbers in the legend denote test conditions, T_{ID} (°C)/T_{OD} (°C)).

overcharging, the higher levels of subcooling had minor effects upon capacity. For the studied subcooling fault range of 0%–181% of the nominal value, outdoor unit power increased by 15%.

4. Concluding remarks

The performance characteristics of a residential split heat pump operating in the cooling mode under various single fault conditions was characterized by normalized values of key performance parameters. In addition, correlations for these normalized values were developed using air temperatures and fault level as independent variables. Dew point temperature was removed as an independent variable in some of the correlations to aid in the prediction of faulty performance outside of the range of experimental data especially in dry climate conditions. Uncertainty of the faulty performance parameters was characterized by an example calculation of COP and total capacity at 10% reduced indoor air flow rate.

Cooling capacity was most affected by the compressor/reversing valve leakage fault and refrigerant undercharge. The undercharge fault is more likely to occur in the field, and thus is the more important fault to monitor. Compressor valve or four way reversing valve leakages would not occur at fault levels higher than 10% unless a reversing valve failed to operate properly. Most normalized values changed linearly with fault level; therefore, it is possible to simulate these types of single faults using simple linear correlations. In the future, it would be helpful to develop these types of correlations for multiple, simultaneous faults because some of the faults studied here do happen at the same time.

References

[1] M.C. Comstock, J.E. Braun, E.A. Groll, The sensitivity of chiller performance to common faults, HVAC&R Res. 7 (2001) 263–279.

[2] M. Kim, W.V. Payne, C.J.L. Hermes, P.A. Domanski, Performance of a Residential Heat Pump Operating in the Cooling Mode with Single Faults Imposed, NISTIR 7350, Natl. Inst. of Stds. Techn., Gaithersburg, MD, USA, 2006.

[3] M. Kim, W.V. Payne, P.A. Domanski, S.H. Yoon, C.J.L. Hermes, Performance of a residential heat pump operating in the cooling mode with single faults imposed, Appl. Therm. Eng. 29 (2009) 770–778.

[4] B. Chen, J.E. Braun, Simple rule-based methods for fault detection and diagnostics applied to packaged air conditioners, ASHRAE Trans. 87 (2001) 771–782.

[5] J. Navarro-Esbri, E. Torrella, R. Cabello, A vapour compression chiller fault detection technique based on adaptive algorithms, application to on-line refrigerant leakage detection, Int. J. Refrig. 29 (2006) 716–723.

[6] M. Kim, S.H. Yoon, W.V. Payne, P.A. Domanski, Cooling Mode Fault Detection and Diagnosis Method for a Residential Heat Pump, NIST Spec. Publ. 1087, Natl. Inst. of Stds. Techn., Gaithersburg, MD, USA, 2008.

[7] M. Kim, S.H. Yoon, P.A. Domanski, W.V. Payne, Design of a steady-state detector for fault detection and diagnosis of a residential air conditioner, Int. J. Refrig. 31 (2008) 790–799.

[8] S. Wang, Q. Zhou, F. Xiao, A system-level fault detection and diagnosis strategy for HVAC involving sensor faults, Energy Build. 42 (2010) 477–490.

[9] S.H. Cho, Y. Hong, W. Kim, M. Zaheer-uddin, Multi-fault detection and diagnosis of HVAC systems: an experimental study, Int. J. Energy Res. 29 (2005) 471–483.

[10] H. Li, J.E. Braun, Decoupling features and virtual sensors for diagnosis of faults in vapor compression air conditioners, Int. J. Refrig. 30 (2007) 546–564.

[11] Z. Du, X. Jin, Multiple faults diagnosis for sensors in air handling unit using Fisher discriminant analysis, Energy Convers. Manag. 49 (2008) 3654–3665.

[12] AHRI Standard 210/240, Performance Rating of Unitary Air-Conditioning and Air-Source Heat Pump Equipment, Air-Conditioning, Heating, and Refrigeration Inst., Arlington, VA, USA, 2008.

[13] ANSI/ACCA Standard 5, HVAC Quality Installation Specification, Air Conditioning Contractors of America, 2007, 2800 Shirlington Road, Suite 300, Arlington, VA 22206, USA.

[14] M. Kim, S.H. Yoon, W.V. Payne, P.A. Domanski, Development of the reference model for a residential heat pump system for cooling mode fault detection and diagnosis, J. Mech. Sci. Technol. 24 (2010) 1481–1489.

[15] M. Farzad, D. O'Neal, System performance characteristics of an air conditioner over a range of charging conditions, Int. J. Refrig. 14 (1991) 321–328.